SUPPLEMENTAL INFORMATION

Supplementary Data

Supplementary Fig. 1 is related to Fig. 1.

Supplementary Fig. 2 is related to Fig. 2.

Supplementary Fig. 3 is related to Fig. 3.

Supplementary Fig. 4 is related to Fig. 4.

Supplementary Fig. 5 is related to Fig. 5.

Supplementary Fig. 6 is related to Fig. 6.

Supplementary Tables S1-S5.

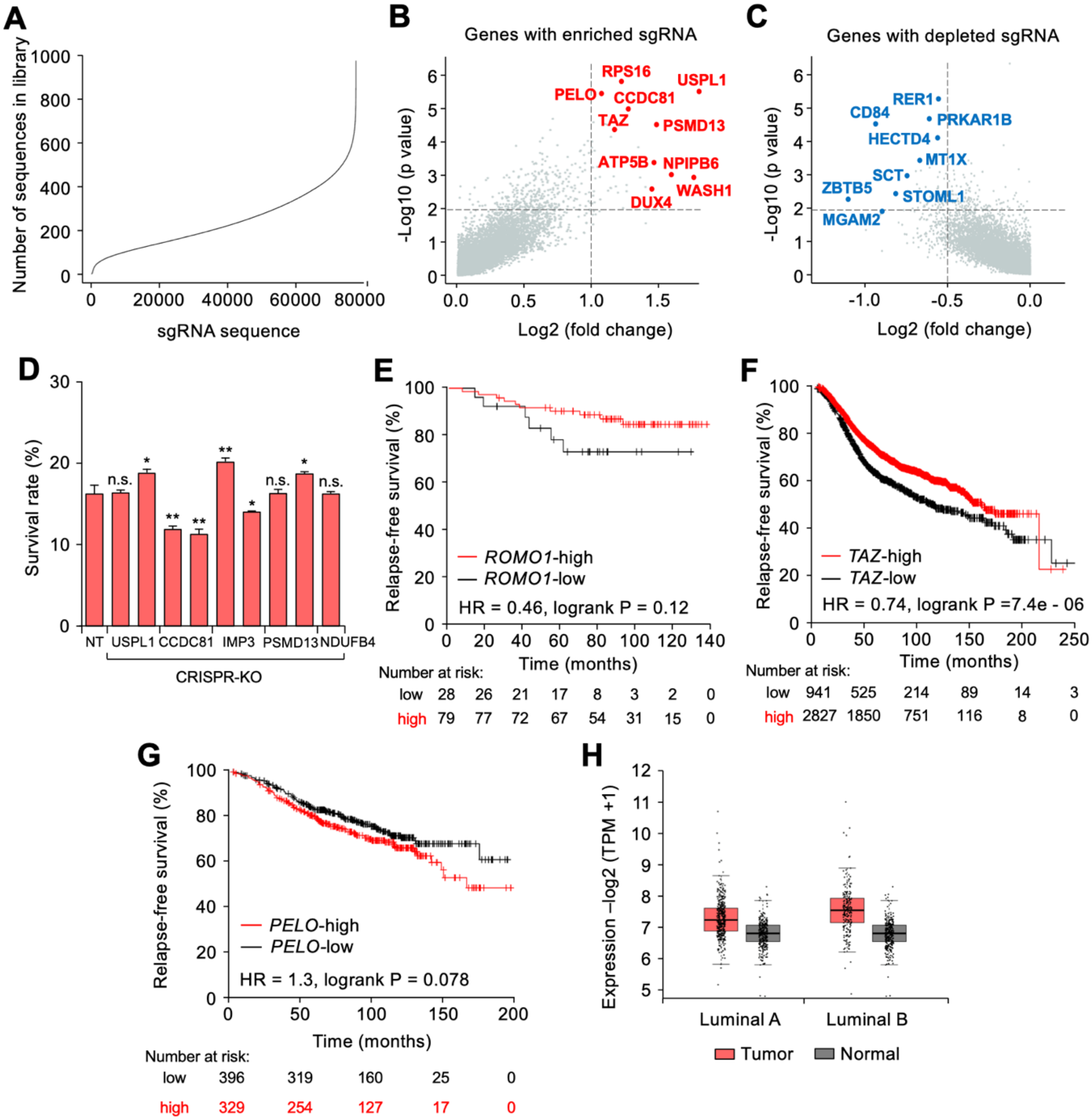

Figure S1. The expression and survival analysis of candidate genes in patient datasets, related to Figure 1. A. The initial quality check of sgRNA library was performed by analyzing the distribution of sgRNAs in sgRNA library transduced cell population, which was used in later screening. **B.** Top candidate genes for enriched sgRNAs. Candidates were plotted based on mean log2 fold change and P values computed by MaGeCK. **C.** Top candidate genes for depleted sgRNAs. Candidates were plotted based on mean log2 fold change and P values computed by MaGeCK. **D.** Several candidate genes were selected and the stable KO of these genes were generated in MCF7 cells. Cells were treated with DMSO or 12 μM tamoxifen for 48

h. The cell survival rate for each group was presented. n = 3 per group, data presented as mean ± SD. n.s. represents no significant difference, * $p < 0.05$, ** $p < 0.01$ by Student’s t-test. **E.** Kaplan-Meier survival plot shows the correlation between the mRNA expression of *ROMO1* and the relapse-free survival (RFS) of ER+ breast cancer patients with tamoxifen therapy based on an online database (https://kmplot.com). **F.** Kaplan-Meier survival plot shows the correlation between the mRNA expression of *TAZ* and the relapse-free survival (RFS) of ER+ breast cancer patients based on an online database (https://kmplot.com). **G.** Kaplan-Meier survival plot shows the correlation between the mRNA expression of *PELO1* and the relapse-free survival (RFS) of ER+ breast cancer patients with tamoxifen therapy based on an online database (https://kmplot.com). **H.** The mRNA expression level of *ROMO1* is higher in breast tumor tissues compared to normal tissues in both Luminal A and Luminal B subtypes of breast cancers. Data was analyzed based on TCGA and GTEx data set on GEPIA2 (http://gepia2.cancer-pku.cn). TPM, Transcripts per million.

A

MCF7 TIDE analysis	
sgRNA	total efficiency (%)
1	76.9
2	88.8
3	26.8

B

T47D TIDE analysis	
sgRNA	total efficiency (%)
1	91.7
2	91.4
3	23.6

C

ZR-75-1 TIDE analysis	
sgRNA	total efficiency (%)
1	82.4
2	79.3
3	16.7

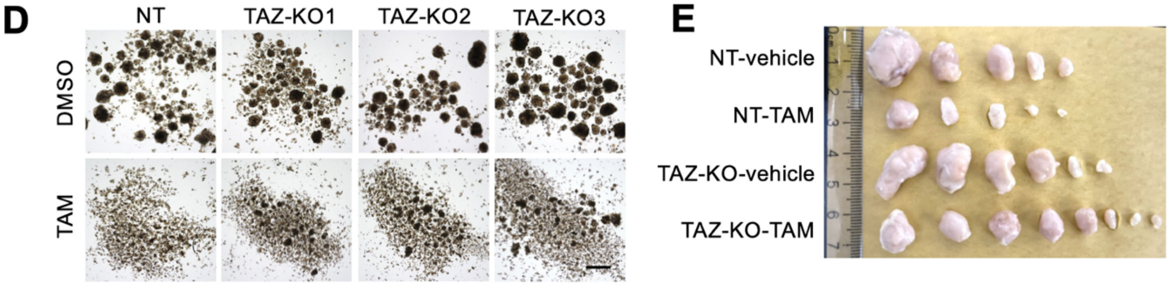

F

MDA-MB-231 TIDE analysis	
sgRNA	total efficiency(%)
1	89.2
2	91.1
3	66.9

G

SCP2 TIDE analysis	
sgRNA	total efficiency(%)
1	93.2
2	87.7
3	49.6

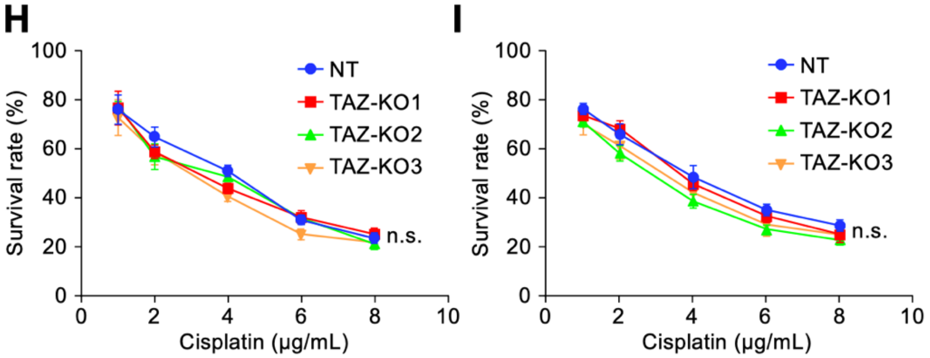

Figure S2. Loss-of-TAZ has little effect of therapy resistance in ER-negative breast cancer, related to Figure 2. A-C. TAZ KO in MCF7 (A), T47D (B) and ZR-75-1 (C) cells using 3 independent sgRNAs were performed and the KO efficiencies were analyzed by TIDE assay. **D.** Representative images of the tumor spheres in Fig. 2D. Scale bar, 50 μm. **E.** Representative images of the tumors in Fig. 2F. **F, G.** TAZ KO in MDA-MB-231 (D) and SCP2 (E) cells using 3 sgRNAs were performed and the KO efficiencies were analyzed by TIDE assay. **H.** NT control and TAZ-KO MDA-MB-231 cells were treated with PBS or increasing concentrations of cisplatin for 24-48 h. The cell survival rate for each group was plotted. n = 3, data presented as mean ±

SD. n.s. represents no significant difference by t-test. **I.** NT control and TAZ-KO SCP2 cells were treated with PBS or increasing concentrations of cisplatin for 24-48 h. The cell survival rate for each group was plotted. n = 3, data presented as mean ± SD. n.s. represents no significant difference by t-test.

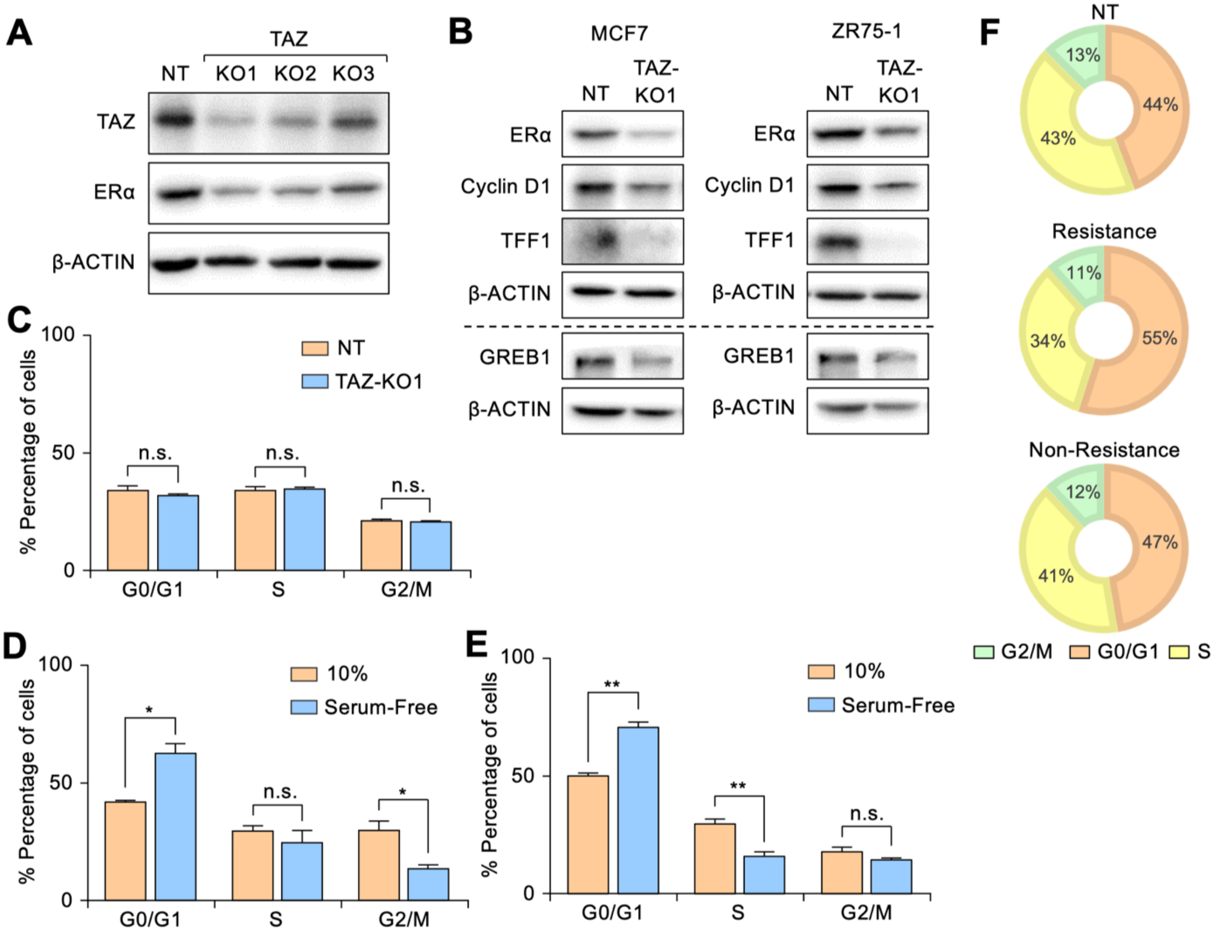

Figure S3. Cell cycle-arrest positively correlates with therapy resistance, related to Figure 3. A. The protein expression levels of TAZ and ERα in NT control and three independent TAZ-KO ZR-75-1 cells were determined by immunoblotting. β-ACTIN was used as the internal loading control. **B.** The expression levels of indicated proteins in NT control and TAZ-KO MCF7 (left) and ZR-75-1 (right) cells were determined by immunoblotting. β-ACTIN was used as the internal loading control. **C.** Cell cycle analysis by PI staining and FACS analysis of NT control and TAZ-KO SCP2 cells. n = 3, data presented as mean ± SD, n.s. represents no significant difference by Student's t-test. **D, E.** Cell cycle analysis by PI staining and FACS analysis of MCF7 (C) and T47D (D) cells cultured in media containing indicated concentrations of FBS for 24 h**.** n = 3, data presented as mean ± SD, n.s. represents no significant difference, * $p < 0.05$, ** $p < 0.01$ by Student's t-test. **F.** The average cell cycle distribution of NT control, tamoxifen-resistant cells (resistance ratio > 1.5) or non-resistant cells (resistance ratio < 1.5) defined by our screening based on experiment in Fig. 3G.

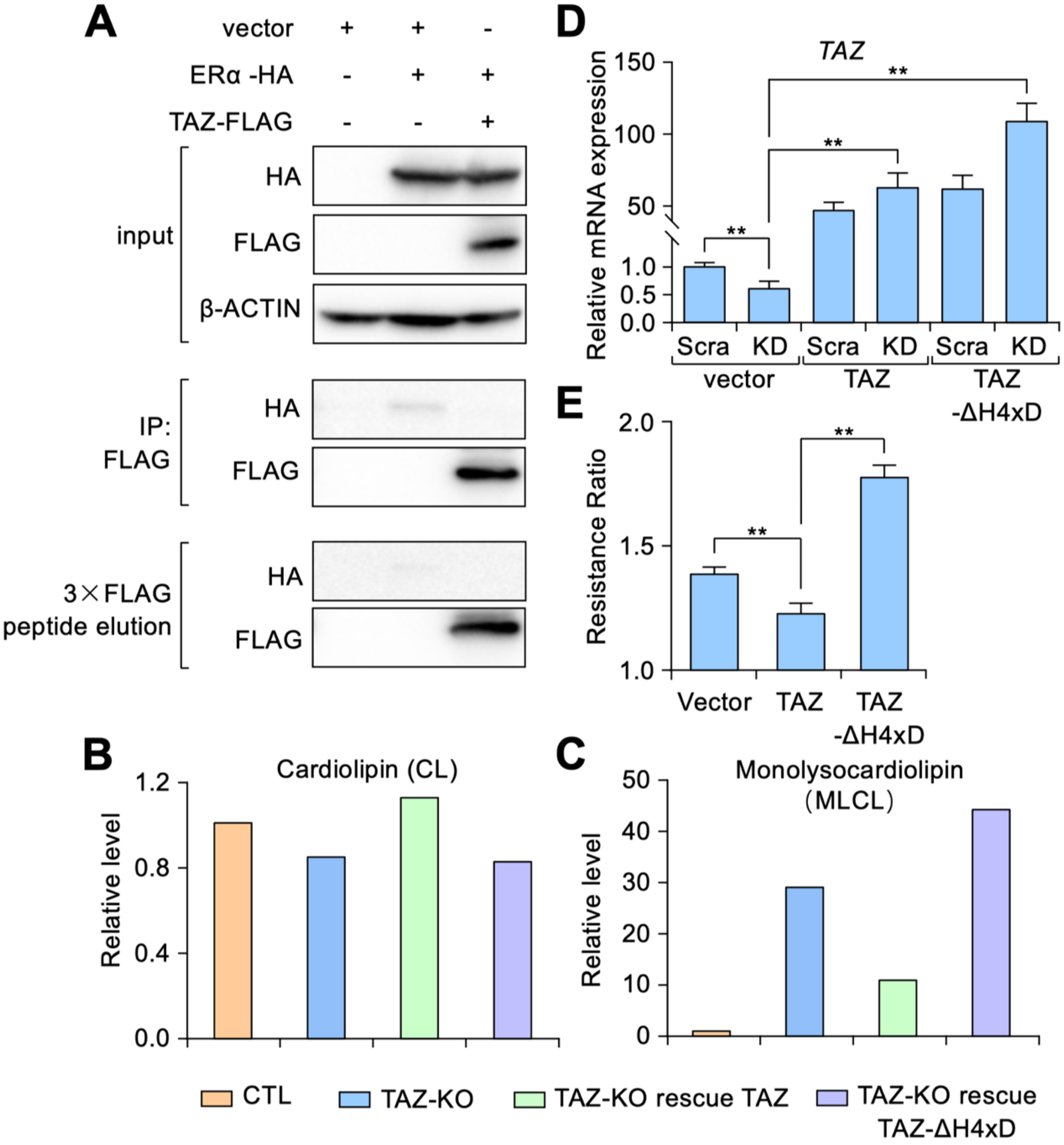

Figure S4. TAZ affects tamoxifen resistance through its enzymatic activity, related to Figure 4. A. HEK293T were transfected with indicated expression vectors. Cells were lysed for immunoprecipitation with α-FLAG antibody for TAZ detection and α-HA antibody for ERα detection. **B, C.** The levels of CL (B) and MLCL (C) were detected using HPLC in TAZ-KO MCF7 cells with either wild type TAZ or TAZ-ΔH4xD mutant rescue. **D.** Endogenous TAZ was KD by shRNA in MCF7 cells, a scramble (Scra) control shRNA was used as control. Wild type TAZ or TAZ-ΔH4xD was re-expressed in either scramble control or TAZ-KD cells. The relative mRNA expression level of *TAZ* was confirmed by qPCR. *GAPDH* was used as the internal control. n = 3, data presented as mean ± SD, ** $p < 0.01$ by Student’s t-test. **E.** Cell lines generated from experiment in B were treated with DMSO or tamoxifen for 48 h. The cell survival ratio for each group was calculated by normalizing to the survival rate of scramble control group. n = 3, data presented as mean ± SD, ** $p < 0.01$ by Student's t-test.

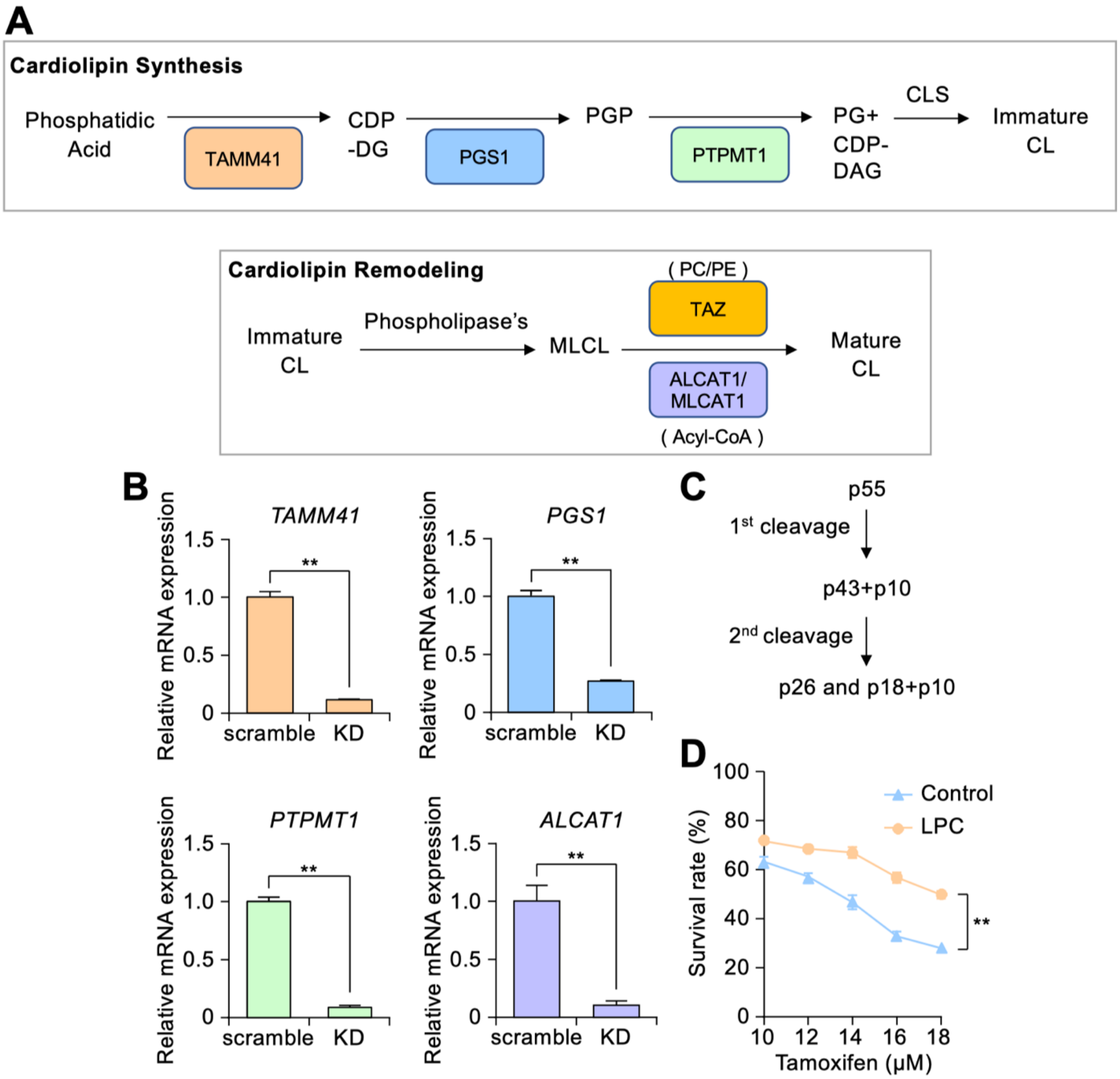

Figure S5. KO of TAZ alters cellular levels of phospholipids and induces tamoxifen resistance, related to Figure 5. A. Schematic representation of phospholipid metabolism pathway leading to mature CL production, in which TAZ utilizes PC or phosphatidylethanolamine (PE) as acyl chain donors to attach to reacylate monolysocardiolipin (MLCL). **B.** KD of CL metabolism-related enzymes in MCF7 cells. The relative mRNA expression levels of these genes were analyzed by qPCR. *GAPDH* was used as the internal loading control. n = 3, data presented as mean ± SD, ** $p < 0.01$ by Student's t-test. **C.** A Schematic illustration of caspase-8 cleavage. **D.** T47D cells were cultured with control vehicle or LPC supplement. Cells were then treated with increasing concentrations of tamoxifen. The cell survival ratio for each group was calculated by normalizing to the survival rate of DMSO-treated control group. n = 3, data presented as mean ± SD. ** $p < 0.01$ by t-test.

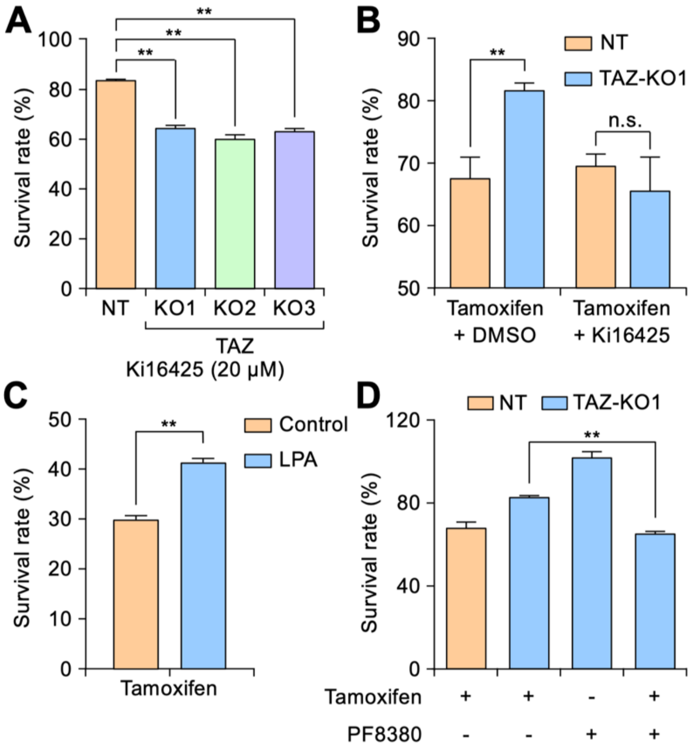

Figure S6. Blockade of the LPA synthesis axis attenuates tamoxifen resistance, related to Figure 6. A. NT control or three independent TAZ-KO MCF7 cells were treated with 20 μM Ki16425 for 48 h. The cell survival ratio for each group was calculated by normalizing to DMSO control group. n = 3, data presented as mean ± SD. ** $p < 0.01$, by Student's t-test. **B.** NT control or TAZ-KO T47D cells were treated with 10 μM tamoxifen alone or in combination with 20 μM Ki16425 for 48 h. The cell survival ratio for each group was calculated by normalizing to DMSO control group. n = 3, data presented as mean ± SD. n.s. represents no significant difference, ** $p < 0.01$, by Student's t-test**. C.** Cell viability of MCF7 under 10 μM tamoxifen treatment, supplemented with vehicle control or LPA. Data presented as mean ± SD. ** $p < 0.01$ by Student's t-test. **D.** NT control or TAZ-KO T47D cells were treated with 10 μM tamoxifen alone, 20 μM PF8380 alone, or in combination of tamoxifen and PF8380 for 36 h. The cell survival ratio for each group was calculated by normalizing to DMSO control group. n = 3, data presented as mean ± SD. n.s. represents no significant difference, ** $p < 0.01$ by Student's t-test.

Table S1. sgRNA sequences used for validation of tamoxifen-resistance candidate genes from the initial screen, related to Methods.

Target Gene	sgRNA sequence (5‘-3’)
Non-Targeting	AAAAAGCTTCCGCCTGATGG
TAZ-sg1	CCTGACCGTGCACAACAGGG
TAZ-sg2	GAATTCCTGCGTTTCAAGTG
TAZ-sg3	GAGATGGCGTCTACCAGAAG
RPS16-sg1	ACAGAAGACAGCGACAGCTG
RPS16-sg2	ATCCGTGTCCGTGTAAAGGG
PELO-sg1	ACTGCTCCCTCACAAATCCT
PELO-sg2	TGACTAAGCAGATATGGGCG
NDUFB4-sg1	CATATCTCCGGAAACCCGGC
NDUFB4-sg2	CAGGTACTCTCGTTTCAGCT
IMP3-sg1	GCGCAGCTTGAGGAGCACGG
IMP3-sg2	AGCTCCAGCGAACCGCGCGT
ROMO1-sg1	ACGGTCGAAGCAGCTTGGCT
ROMO1-sg2	CTCCTCAGGATCGGAATGCG
PSMD13-sg1	ATGAAGAATGATTTCCACGA
PSMD13-sg2	GAACCGATGTCACACCAGGA
USPL1-sg1	CCTAATGTGCATCTAAGCTG
USPL1-sg2	GTCCTGTGAAAGAGTACGAG
CCDC81-sg1	AGCTTGCCAGGATCATAACA
CCDC81-sg2	TTCTCCACCATGATAAACAC

Table S2. Primers used for qPCR and PCR gene cloning, related to Methods.

Gene	Forward (5‘-3’)	Reverse (5‘-3’)
qPCR primers		
GAPDH	GGAGCGAGATCCCTCCAAAAT	GGCTGTTGTCATACTTCTCATGG
TAZ	CACCGTGTCCAATCACCAGTC	TCCAACGCATCAACTTCAGGT
CCND1	GCTGCGAAGTGGAAACCATC	CCTCCTTCTGCACACATTTGAA
ESR1	GGGAAGTATGGCTATGGAATCTG	TGGCTGGACACATATAGTCGTT
GREB	ATGGGAAATTCTTACGCTGGAC	CACTCGGCTACCACCTTCT
MYC	GGCTCCTGGCAAAAGGTCA	CTGCGTAGTTGTGCTGATGT
PGR	TTATGGTGTCCTTACCTGTGGG	GCGGATTTTATCAACGATGCAG
TFF1	CCCCGTGAAAGACAGAATTGT	GGTGTCGTCGAAACAGCAG
TFF2	GCTGTTTCGACTCCAGTGTCA	CCACAGTTTCTTCGGTCTGAG
TFF3	CCAAGCAAACAATCCAGAGCA	GCTCAGGACTCGCTTCATGG
TAMM41	CAGTAGATGACCCTGTCGCAT	GGATGGACGTGATAATCTTGGG
PGS1	TCGTGATGGCATCCCTCTAC	CCCCGCGTGAAGTCTAAGA
PTPMT1	CAGAGGAGGCTGTAAGAGCCA	TGTGGATGTATGACCGGATCT
ALCAT1	CACCCTACCTGTGGCATTATTG	CCATTCTTGTCCGATGGTTCAT
ATX	ACTTTTGCCGTTGGAGTCAAT	GGAGTCTGATAGCACTGTAGGA
PCR primers		
TAZ	ATGCCTCTGCACGTG	CTATCTCCCAGGCTGGAG
ESR1	ATGACCATGACCCTCCACACC	TCAGACCGTGGCAGGGAAACCC

Table S3. shRNA sequences used in the study, related to Methods.

Target Gene	shRNA sequence (5‘-3’)
Scramble	CCTAAGGTTAAGTCGCCCTCG
TAZ-sh1	CGGACTTCATTCAAGAGGAAT
TAZ-sh2	CTGTACGAGCTCATCGAGAAG
TAMM41	GACTTTGTGTTCACAGTAGAT
PGS1	GCCTGGAAAGTACTCTAGAAA
PTPMT1	GATCCGGTCATACATCCACAT
ALCAT1	CAGTCTTGTTAAGTGGTATTT

Table S4. TIDE analysis of candidate genes. Related to Figure 1.

Gene	Wt	Ko	Efficiency
PELO-sg1	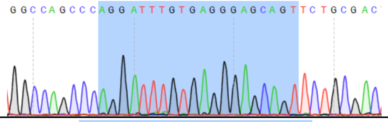	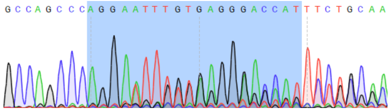	63.6
PELO-sg2	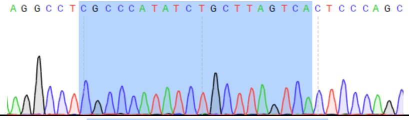	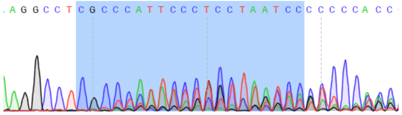	35.4
ROMO1-sg1	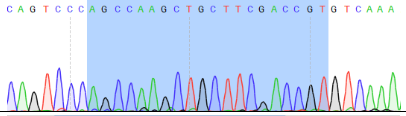	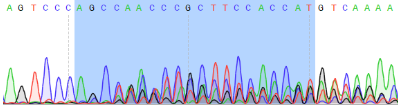	35.2
ROMO1-sg2	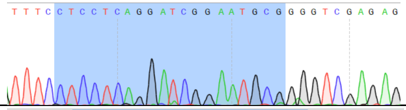	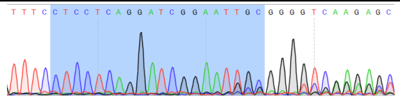	9.9
TAZ-sg1	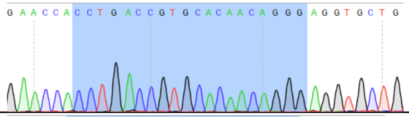	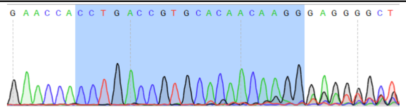	76.9
TAZ-sg2	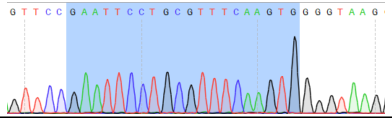	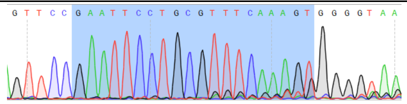	88.8
USPL1-sg1	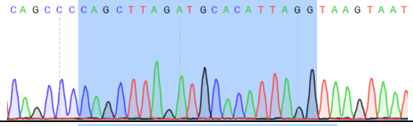	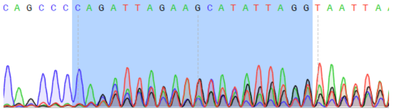	49
USPL1-sg2	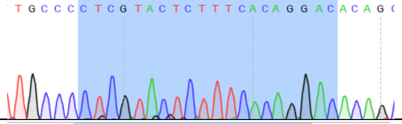	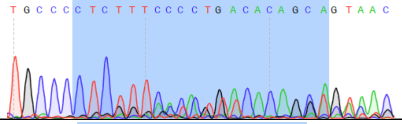	85.9
CCDC81-sg1	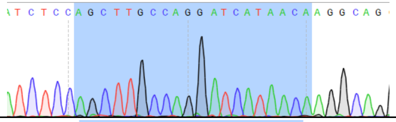	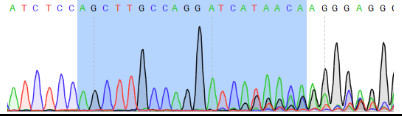	18.5
CCDC81-sg2	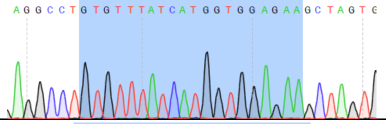	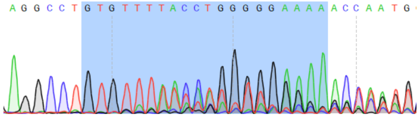	57.2
IMP3-sg1	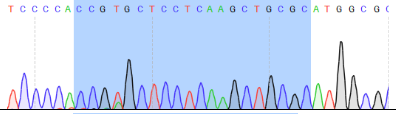	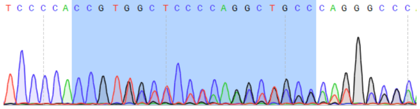	61.7
IMP3-sg2	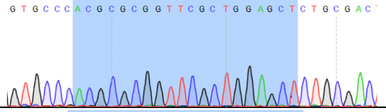	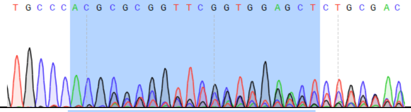	48.4
PSMD13-sg1	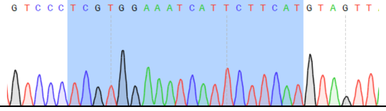	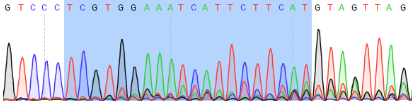	34.7

PSMD13-sg2	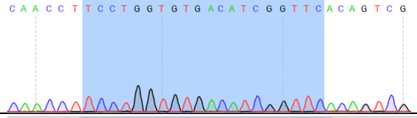	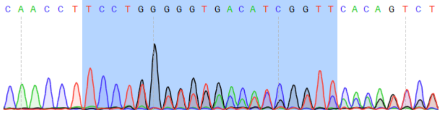	33.1
NDUFB4	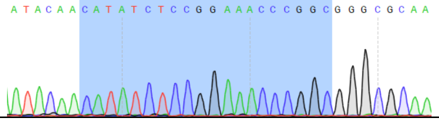	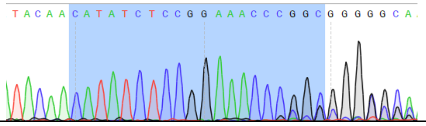	52.6

Table S5. sgRNA sequences for correlation analysis of cell proliferation index and tamoxifen resistance index, related to Figure 3.

Gene symbol	sgRNA sequence (5‘-3’)	Proliferation Index	Resistance Index
Low-proliferation			
MTOR (sg1)	GGTGATGGCCTGGACAACCA	0.15	1.57
PSMB2	TTTATAAGATGCGAAATGGT	0.23	1.68
WASH1	GGTGGTGTTGAAGAGCAGCA	0.26	1.38
EIF3CL	GCAGAGCATGGTGGTAGATG	0.30	2.35
MTOR (sg2)	TCAGGAAATGATCCGCACAG	0.31	1.43
PPP1R7	GCTGGGATCTAACCGCATCC	0.32	0.75
RPS12	TCCACCAACTTGACATACAT	0.34	1.13
NOTCH2NL (sg1)	GGGATGAGACAGGCAGGCAT	0.35	1.30
EXOSC8	GGAAATACTACAGTAATCTG	0.35	1.63
SOD1	GGAAAGTAATGGACCAGTGA	0.38	1.49
PSMD13	ATGAAGAATGATTTCCACGA	0.41	1.79
USP7	GGCAACCTTTCAGTTCACTG	0.47	1.69
NF1	GAGGAAGCAGATATCCGGTG	0.47	1.56
SARS2	TACCGGGCAGAGACAAACAC	0.48	2.10
Medium-proliferation			
NOTCH2NL (sg2)	TCTCGACCTTGCCTGAATGG	0.51	0.98
EXOC4	TTCTCATAGATGAACTACAC	0.51	1.60
PIK3C3	AGCCTGCAAAAACTCAACAC	0.57	1.19
USPL1	CCTAATGTGCATCTAAGCTG	0.57	1.24
MOCS3	AATCTCATCTCGGGACAGAG	0.63	1.51
GATA1	GCGGGTGGGACACACAGTTG	0.68	0.98
AURKA	CCATATAGAAAATAATCCTG	0.72	1.09
CIB3	AAGGTGCCCTACGAGCTCAT	0.74	0.93
CGB1	GCATTGATGGGGCGGCACCG	0.76	0.97

NOL7	GGCGAAAGTCAGCTCCTCCG	0.80	1.40
TAZ	CCTGACCGTGCACAACAGGG	0.88	2.13
LATS1	CCTTCTGCTTTACAAACAGG	0.89	1.18
RAB9B	CTTAGGACACCCTTCTACAG	0.92	1.12
CCDC81	AGCTTGCCAGGATCATAACA	0.98	0.90
High-proliferation			
CNNM3	ATGGTTGTAGAAACGAGTGA	1.24	1.33
GOLPH3	TGTATATCATCTGGATTACG	1.37	1.16
MRAS	GGAGCAATACATGCGCACGG	1.50	1.24